Dispatch-Oriented Thermo-Economic Design of a 50 MW Parabolic Trough Solar Plant for Mandalgobi Cold-Climate Operation

Jawad Javed[1,*] and Maria Jawad[1]

[1] IU International University of Applied Sciences
* Correspondence: b.jawad4891@gmail.com

Abstract: Annual energy yield and levelized cost are popular ways to evaluate dispatchable concentrating solar power, but the limitations that emerge for thermal-oil parabolic trough plants located in cold semi-arid locations are overlooked by these aggregated performance indicators. What is proposed in this investigation is a coordination among the sizes of solar-field aperture, amount of thermal-energy-storage, and a forecast-driven supervisory plant control strategy to mitigate seasonal energy imbalance, part load operation, and cost increase in a 50 MW parabolic trough concentrating solar power plant in Mandalgobi, Mongolia. The plant characteristics considered are the EuroTrough-150 collectors, Therminol VP-1 heat-transfer fluid, indirect two-tank molten salt thermal energy storage, reheated Rankine cycle, design direct normal irradiance of 0.80 kW m^{-2}, heat-transfer-fluid temperatures of 280/395 °C, solar field efficiency of 67.4%, power block efficiency of 35.72%, and overall solar-to-electric conversion efficiency of 22.03%. According to the results for the seasons, significant seasonal imbalance is observed due to the lack of charge capacity in the storage during the cold months. For example, on March, June, September, and December, the plant generates 580.12, 867.64, 511.76, and 105.31 MWh of electric energy, respectively. Also, storage makes 107, 295, and 75 MWh contribution on the corresponding days, but it has almost no value in winter due to insufficient charging opportunities of the field. On this basis, the methodology integrates seasonal analysis, multi-criteria sizing of solar-field aperture and thermal-energy storage, as well as a receding-horizon controller which sets the heat-transfer fluid flow rate, thermal-energy-storage charges-discharges, and loading of the turbines. According to the findings, the summer day yields 8.24 times more energy than the December one, whereas storage provides 34.00% of electric power on the summer day and only 14.66–18.44% during shoulder seasons. The economic optimum of the solar-field aperture changes from the reference value of 261,600 m^2 to 523,200 m^2 at the solar multiple of 2.0 and LCOE of USD 0.2143 kWh^{-1}. It can be concluded that cold weather trough dispatchability cannot be attained simply because of storage capacity, but rather it requires a sufficient area for the creation of charge opportunities as well as supervision of these opportunities to stabilize turbine operations.

Keywords: parabolic trough concentrating solar power; cold-climate operation; thermal energy storage; solar multiple; model predictive control; thermo-economic optimization; off-design power block

Citation: Jawad Javed and Maria Jawad. 2022. Dispatch-Oriented Thermo-Economic Design of a 50 MW Parabolic Trough Solar Plant for Mandalgobi Cold-Climate Operation. *TK Techforum Journal (ThyssenKrupp Techforum)* 2022(2): 97–119.

Received: February-27-2022
Accepted: Augsut-21-2022
Published: September-30-2022

1. Introduction

The reduction of greenhouse gas emissions has made renewable power sources with controllable output more valuable than simply those which supply energy with variability. The significance of concentrating solar power (CSP) lies in the conversion of solar radiation to thermal energy which allows the storage of thermal energy (TES) and the use of turbogenerators in synchronous fashion [1–4]. Line-focusing CSP based on the use of parabolic trough collectors (PTCs) is still the largest CSP installation by power rating worldwide, due to the engineering proof provided by its optical design, evacuated receiver tube construction, thermal oil circuit, and the integration of a Rankine cycle [5–7]. Cost and

best practice analyses have additionally established that the performance of trough power stations depends heavily on their integration, commissioning procedure, receiver losses, parasitics, and availability rather than on the efficiency of the solar field alone [8,9].

The well-developed technology base of PTCs does not eliminate the importance of optimization in the case of a specific installation. Aperture area, collector circuits, heat loss from the receiver, HTF temperature, storage capacity, steam generation characteristics and efficiency, and parasitic cooling load all influence the yearly profitability of an installation [10–13]. While a configuration may appear efficient at full design capacity, it can prove unviable if it leaves the generator inadequately supplied during partial operation, if the storage system cannot be recharged on winter days, or if the dispatch regime forces the power block into inefficient part-load operation. Thermal-oil trough designs have an additional complexity since their components react on different time-scales and according to different physics laws.

The optics and thermodynamics of troughs have been well explored in previous literature. Experiments and analytical heat transfer analyses of receivers revealed loss modes associated with absorber tubes and the impact of fluid temperature, winds, incidence angle, and annular conditions on net heat collection. Literature reviews of trough geometry, tracking, optical efficiency, receiver technologies, and applications followed. Research on TES demonstrated that an indirect two-tank molten salt TES can enhance dispatchability, but only when sufficient excess energy from the solar field exists to fill the two tanks post-power block demand. Together, this literature establishes the physical basis of trough components, but it is not sufficient for determining the optimal trade-off between excess solar field capacity, storage capacity, and plant control for a cold climate.

A second literature line has been devoted to annual performance analysis, cost-benefit assessments, and plant dynamics simulations. The physical trough modeling framework implemented within the System Advisor Model (SAM) accounts for the performance of the solar field, HTF piping, thermal storage, power block, auxiliary heat, and plant control through an engineering model suited for assessing the performance and economics of such plants [14]. Studies in techno-economics have studied the sensitivity of trough plants to solar multiple, duration of thermal storage, dry cooling, HTF type, and site-dependent solar characteristics [15–18]. Dynamic analysis of plants has revealed the influence of transient behaviors associated with steam generation, storage, and power block start-ups [19–22]. This suggests that annual performance is an inherently dynamic quantity.

Moreover, the same literature points out that environmental effects vary the importance of each subsystem loss. According to dry-cooling studies, the amount of water available and the efficiency of heat rejection by the condenser depend on ambient temperature, influencing net power production and electricity cost [23]. In addition, exergy analyses of trough-integrated cycles suggest that exergy destruction occurs across multiple system interfaces such as solar radiation concentration, heat exchange from collector fluid to working fluid, steam generation, and steam expansion through the turbine [24]. In addition, the study of HTF performance adds another restriction since oil thermal characteristics, allowable temperature range, viscosity, and stability constrain how actively the solar field operates after the initial cold start [25]. Therefore, Mandalgobi's situation requires a solution far beyond collecting a few more sun-hours. The power plant needs to generate sufficient thermal energy of appropriate temperature quality, ensure a low share of auxiliary energy consumption, and operate in a power-block regime where thermal input would be highly productive.

Off-design regime explains why design and control cannot be treated independently. Although some designs satisfy energy balance requirements at their rated operating capacity, they could perform suboptimally for most of the operating period due to factors like low DNI levels, incidence angles, heat losses from receivers, cloud cover disruptions, and heat tracing during the winter months [26,27]. Thermal energy storage (TES) can help to cope with such problems, but the TES itself does not provide any additional source of energy and merely redistributes the heat generated by the solar field. As a result, the

cost-effectiveness of the storage is determined by several parameters such as solar multiple, opportunity to charge, dispatch time horizon, and operational strategy [28–30].

The coupling becomes more critical in cold semi-arid environments. One illustrative example at the plant scale comes from Mandalgobi, Mongolia, due to the presence of both significant seasonal variation in radiation availability as well as cold weather during winter and a low-angle solar path, which limits winter collection capacity. The Mandalgobi 50 MW trough plant design data provides a solar-field efficiency of 67.4%, power-block efficiency of 35.72%, and overall solar-to-electric efficiency of 22.03% at the design point, with severe seasonal variation between June and December operations [31]. In addition, the optimal aperture size is about 523,200 m^2, representing solar multiple 2.0 and corresponding to minimum LCOE of 0.2143 USD/kWh^{-1}, whereas the reference solar field has 80 loops and 261,600 m^2. This difference in sizing does not represent a minor detail but rather indicates that the reference solar field is undersized for the purpose of charging the storage capacity.

The control literature further justifies the presence of supervisory level control. Model Predictive Control (MPC) technology is widely applied in industrial processes because it takes into account the constraint handling, multivariable interaction, prediction horizon, and actuators' limitations [32–34]. For solar troughs, MPC appears particularly applicable since the collector field exhibits thermal inertia, and the outlet HTF temperature needs to stay within narrow bounds. Moreover, the disturbance related to DNI arrives at the power block with a certain time delay [35]. It is thus appropriate to consider field sizing, storage scheduling, and power block loading as one control-design problem.

Another unresolved issue that comes out of this literature is the lack of integration between field-sizing and operational considerations. Many papers optimize the solar multiple or storage hours through an annual simulation, while many others develop controllers for CSP assuming a physical system that is already sized optimally. This distinction can lead to distorted results. If a system is sized based on weak assumptions regarding operations, the resulting field size will not produce sufficient excess thermal power for the controller to utilize. If one then develops a controller for such an undersized system, the benefit of the control scheme will be minimal because a larger field could yield greater storage contribution. On the other hand, if a larger system is built, its economic evaluation will incorporate heat production that cannot be used for charging storage. A cold-climate plant exacerbates this issue because winter operation constrains solar energy availability while summer operation limits the utilization of excess energy [9,18,31].

In this context, the use of Mandalgobi as a CSP diagnostic test case is valuable because the separation of effects is possible. The design-point characteristics allow testing whether the CSP technology chosen makes sense thermodynamically. Seasonal operating days will check whether this configuration will remain dispatchable when the system operates under varying conditions in winter and summer. Storage contributions will verify whether the system is bound by storage tank capacity or the opportunity to fill storage. Field size will examine whether the economic optimal system size will match the physical limitations on charge opportunity. Finally, the supervisory control law development will examine what kind of information is needed to make additional energy collected from the field usable.

The research question for the current paper is: how can solar field sizing, TES application, and predictive supervisory control be optimized in combination to enhance dispatchability and economics of operation of a 50 MW parabolic trough CSP plant at the cold-climate Mandalgobi site? This research question is distinct from a traditional design point analysis because its answer is assessed by the criteria of generation imbalance per season, storage contribution, part load risk, and size of the solar field rather than by efficiency at nominal point. It is also distinct from an optimal control question because the controller in consideration is implemented at the very stage of optimization of a CSP plant size.

The unique feature of the approach taken is that Mandalgobi site data become connected to a design-control analysis argument. The design point parameter values, four sample operating days, contribution of storage to power generation, result of solar field size

calculation, and LCOE figure are all seen as an integrated evidence base rather than just numerical parameters. The sizing task involves solar multiple, aperture area, storage duration, HTF outlet temperature, and number of loops relative to annual energy production, auxiliary consumption, heat dumping, LCOE, capacity factor, and winter time operation capability. The supervisory control logic employs DNI forecast as well as air temperature predictions in order to schedule HTF flow, storage charging-discharging process, and power block loading.

The opening visual in Figure 1 captures in one image the physical setting, seasonal operational days, and output imbalances associated with Mandalgobi. The discrepancy between 867.64 MWh in June and 105.31 MWh in December is why the operation of Mandalgobi should not be understood solely based on rated capacity and design-point efficiency. Mandalgobi needs to be designed through a process that acknowledges heat shortage seasonality, charging possibilities, and part-load as correlated characteristics of the same sun resource. This opening therefore sets out the pathway of evidence presented in this paper, whereby the plant first becomes understood as a cold climate energy routing plant, then a seasonal storage challenge, and eventually a coupled field sizing/dispatch issue.

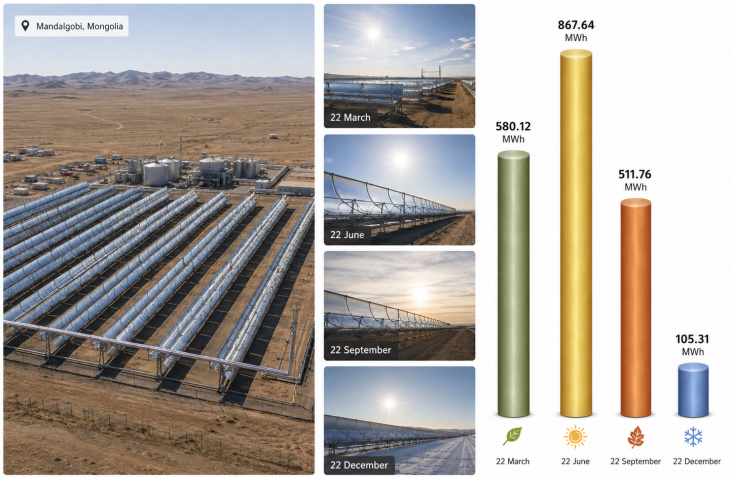

Figure 1. Cold-climate dispatch setting.

2. Plant Configuration and Evidence Base

2.1. Plant configuration

The reference configuration is a 50 MW parabolic trough CSP plant utilizing EuroTrough-150 collector, Therminol VP-1 HTF, an indirect two-tank molten-salt TES system, a sequence of heat exchangers for transferring heat between HTF, salt, and water, and a reheated Rankine power block. In the design point of 0.80 kW m^{-2} DNI, the thermal energy collected from the solar field raises HTF temperature from 280 °C to 395 °C. Then, the thermal energy is either sent to the steam generation sequence or charged into the TES facility as a function of solar surplus and dispatch strategy. The plant consists of 80 collector loops and 261,600 m^2 aperture area [31] (Table 1).

This establishes the thermodynamic envelope inside which the subsequent problem will have to be solved. Given the mass flow rate of the HTF and field temperature rise of 115 °C, the reference solar field may be regarded as a sizable thermal transmission system subject to pumping and heat losses. In this case, a solar-to-electric efficiency of 22.03% must not be taken as a year-round average since it was measured at the nominal point and thus takes no account of inefficiency due to low winter irradiation, recurrent startup, part-load, and inability to charge the storage system.

Steam side values help to understand dispatchability. Main steam parameters of 100 bar, 370 °C and reheated steam parameters of 16.5 bar and 370 °C coupled with exhaust pressure of 0.08 bar show that the considered power plant uses the Rankine

cycle which needs stable thermal inputs to be efficient. It means that main steam and reheated steam mass flow rates of 211.1 t h^{-1} and 169.5 t h^{-1} cannot be diminished without damaging turbine efficiency, heat exchanger approach temperature and auxiliary consumption. Furthermore, feed water temperature of 235 °C implies that steam generation requires an appropriately coordinated set of thermal steps as opposed to a single heat source input. The point is that the controller is not supposed to maximize receiver energy output, but ensure its timely delivery with required parameters to allow efficient thermal energy conversion by the Rankine cycle.

Table 1. Reference plant data.

Parameter	Unit	Value
Gross electric power output	kW	50,000
Main steam pressure	bar	100
Main steam temperature	°C	370
Reheated steam pressure	bar	16.5
Reheated steam temperature	°C	370
Exhaust steam pressure	bar	0.08
Feedwater temperature	°C	235
Main steam mass flow rate	t h^{-1}	211.1
Reheated steam mass flow rate	t h^{-1}	169.5
HTF inlet temperature to solar field	°C	280
HTF outlet temperature from solar field	°C	395
HTF mass flow rate	t h^{-1}	1866
Design-point DNI	kW m^{-2}	0.80
Number of collector loops	–	80
Reference aperture area	m^2	261,600
Solar-field thermal efficiency	%	67.4
Power-block thermal efficiency	%	35.72
Overall solar-to-electric efficiency	%	22.03

Lastly, collector loop and aperture values translate the problem back from thermodynamics to the field size problem. Collector loops numbering 80 and total field area equaling 261,600 m^2 means that each loop receives approximately 3270 m^2 of aperture; thus, the economic optimum of 523,200 m^2 may be seen as a number of roughly 160 reference loops equivalent. Such interpretation may be useful while considering the LCOE optimum because doubling aperture translates directly into doubling physical capacity of the field: more collectors, receivers, piping, HTF inventory, valves, mounts and all other necessary physical resources.

The vertical thermal architecture in Figure 2 explains why the problem being solved cannot be isolated from the rest of the system. The solar field aperture will determine the volume of the heat available for the HTF loop; the oil-to-salt interface and oil-to-water interfaces will determine where the heat can be stored or passed into the steam train, while the Rankine Cycle will determine how valuable the transferred heat will be. In turn, any control effort that alters the HTF flow will have an effect on the collector outlet temperatures, charge possibilities in the store, pumping losses, and turbine load all at once.

From the point of view of conversion at the design point (see Figure 3), it becomes clear that Mandalgobi indeed features a sound rated-state energy balance, but it also identifies where the room for improvement is limited. The solar field's performance level is significantly above the efficiency of solar-to-electric conversion, and thus additional conversion losses and auxiliary energy use have a strong influence on the power generated by the plant. This indicates that improvements to the plant cannot focus solely on the efficiency of the collector field.

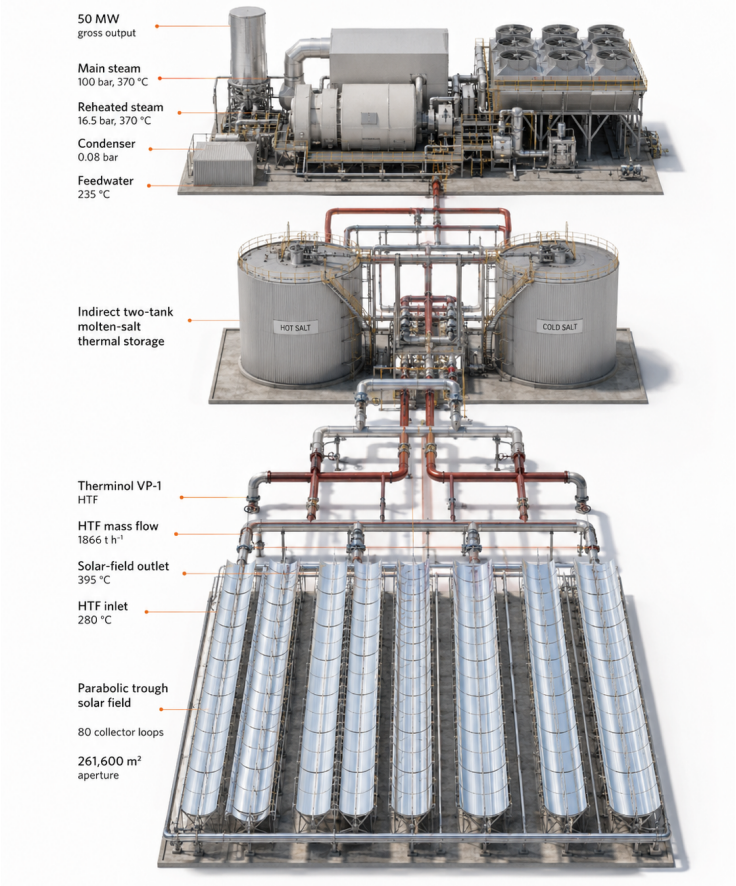

Figure 2. Thermal architecture.

Figure 3. Design-point conversion.

2.1.1. Evidence for seasonal operating cases

This work employs an efficiently condensed set of evidence derived from the plant at Mandalgobi. The evidence includes the design point quantities mentioned above, four seasonal operating days, TES contribution during each day, reference aperture area, the economically optimal aperture area, and the associated minimum of LCOE. The four seasons considered are 22nd of March, 22nd of June, 22nd of September, and 22nd of December. These days have net generation figures of 580.12 MWh, 867.64 MWh, 511.76 MWh, and 105.31 MWh, respectively [31]. The contribution of TES is 107 MWh during March, 295 MWh during June, 75 MWh during September, and zero during December.

The case evidence presented here is not intended as the result of some new measurement campaign. Instead, the case evidence serves to isolate and make explicit the design-control insights of a plant-specific case study. This distinction is critical because the current paper does not attempt to replace a one-year simulation by hour. The purpose of

the presented evidence is to highlight which decisions drive plant performance: the size of the solar field, storage charge opportunities, the part load factor, winter heat margin, and the policy used in allocating heat. The evidence presented in the paper provides sufficient information to state the dispatchability question for cold climates, and it reveals why a nominal-point sizing is insufficient to address this issue.

The evidence included in the four operational days retains the initial seasonal contrast explicitly. The seasonal design question is not derived from any abstraction of weather classes. Instead, it refers to explicitly-stated figures of daily net generation: 580.12 MWh, 867.64 MWh, 511.76 MWh, and 105.31 MWh, and explicitly-stated contributions of storage: 107 MWh, 295 MWh, 75 MWh, and zero MWh. These figures allow us to compute TES share, direct generation share, and output ratio during June-December without resorting to hidden assumptions. Thus, the resulting set of evidence is efficiently condensed and concrete: the plant generates strongly in summer, moderately in shoulder seasons, weakly in winter, and the value of storage follows the availability of surplus rather than the needs of seasonality.

3. Thermo-Economic and Control Formulation

3.1. Solar-field model

For the solar field, useful thermal power is represented by the HTF energy balance

$$Q_{\mathrm{u,SF}}(k) = \dot{m}_{\mathrm{HTF}}(k) c_{p,\mathrm{HTF}} [T_{\mathrm{out}}(k) - T_{\mathrm{in}}(k)], \tag{1}$$

where $\dot{m}_{\mathrm{HTF}}$ is HTF mass flow rate, $c_{p,\mathrm{HTF}}$ is specific heat, and T_{out} and T_{in} are the solar-field outlet and inlet temperatures. The corresponding solar-field efficiency is

$$\eta_{\mathrm{SF}}(k) = \frac{Q_{\mathrm{u,SF}}(k)}{\mathrm{DNI}(k) A_{\mathrm{SF}}}. \tag{2}$$

This mathematical formulation is purposely kept terse, but it encapsulates the key component of the low-temperature effect. As the ambient temperature is low or the incidence angle is bad, more of the heat gained is dissipated away before becoming available enthalpy of the HTF. Higher mass flow rates could ensure that the outlet temperature regulation is maintained, but higher mass flows will require greater pumping efforts while lowering the residence time needed for heating. In this case, the connection between the design parameter, A_{SF}, and the operational variable, $\dot{m}_{\mathrm{HTF}}(k)$, is the first justification for joint field size and control optimization [14].

Solar multiple is defined as

$$\mathrm{SM} = \frac{Q_{\mathrm{SF,des}}}{Q_{\mathrm{PB,des}}}, \tag{3}$$

where $Q_{\mathrm{SF,des}}$ represents the useful solar field thermal power at the design point, and $Q_{\mathrm{PB,des}}$ is the thermal power needed for the power block to operate at the rated capacity. In the current power plant, the reference size of the field is equivalent to an aperture of 261,600 m^2. The economic minimum for the Mandalgobi scenario is around 523,200 m^2, which is double the size of the reference size field. Increasing the aperture size from reference to double the size does not amount to a simple geometrical transformation only.

3.2. Thermal-storage model

The indirect two-tank molten-salt system is described through a storage-energy balance,

$$E_{\mathrm{TES}}(k+1) = E_{\mathrm{TES}}(k) + \eta_{\mathrm{ch}} Q_{\mathrm{ch}}(k) \Delta t - \frac{Q_{\mathrm{dis}}(k)}{\eta_{\mathrm{dis}}} \Delta t - Q_{\mathrm{loss}}(k) \Delta t, \tag{4}$$

with the state constraint

$$0 \leq E_{\mathrm{TES}}(k) \leq E_{\mathrm{TES,max}}. \tag{5}$$

Storage capacity is expressed as equivalent full-load hours,

$$E_{\mathrm{TES,max}} = H_{\mathrm{TES}} Q_{\mathrm{PB,des}}. \tag{6}$$

The trade-off demonstrates the fact that the storage volume by itself cannot serve as an appropriate design criterion. An increased $E_{\mathrm{TES,max}}$ parameter will be of no use if $Q_{\mathrm{ch}}(k)$ will stay low for long intervals during winters. On the contrary, with more solar field available, $Q_{\mathrm{ch}}(k)$ increases during periods of resource abundance; however, it can be wasted in case the controller fails to predict the demand peak at nights or during low-resource intervals. Thus, an effective storage criterion should be the actual pattern of the charge-discharge process [22,28,30].

3.3. Power-block and auxiliary model

Gross power-block efficiency is written as

$$\eta_{\mathrm{PB}}(k) = \frac{W_{\mathrm{gross}}(k)}{Q_{\mathrm{PB}}(k)}, \tag{7}$$

and net output is

$$W_{\mathrm{net}}(k) = W_{\mathrm{gross}}(k) - P_{\mathrm{aux}}(k). \tag{8}$$

Auxiliary components include HTF pumping, salt pumping, electric loads on the cooling system, freeze protection, tracing, and services in the plant. When running at part load, the formula used to calculate the power block will change. The decreased steam production will lead to reduced turbine performance, whereas there is no proportional reduction in auxiliary loads when the amount of net power produced is lower [21,26,27].

Annual net generation and capacity factor are then defined as

$$E_{\mathrm{an}} = \sum_{k \in \Omega} W_{\mathrm{net}}(k) \Delta t, \tag{9}$$

$$\mathrm{CF} = \frac{E_{\mathrm{an}}}{W_{\mathrm{rated}} \times 8760}. \tag{10}$$

In other words, the above formulas illustrate why daily generation numbers cannot be analyzed as standalone values. For instance, a sunny day during the summertime will result in a positive impact on yearly energy generation provided there is no too much dumping. A negative daily number in wintertime will negatively affect the yearly generation number even more if it results in additional start up, freeze protection needs, and periods when the turbine works out of its most effective load range.

3.4. Economic model

The levelized cost of electricity is calculated as

$$\mathrm{LCOE} = \frac{C_{\mathrm{cap}} \mathrm{CRF} + C_{\mathrm{O\&M}}}{E_{\mathrm{an}}}, \tag{11}$$

where C_{cap} is total capital cost, $C_{\mathrm{O\&M}}$ is annual operation and maintenance cost, and E_{an} is annual net electricity generation. The capital recovery factor is

$$\mathrm{CRF} = \frac{r(1+r)^D}{(1+r)^D - 1}, \tag{12}$$

where r is the discount rate and D is the plant lifetime. Cost assumptions follow the example of the Mandalgobi study, using characteristic numbers for the solar field aperture, HTF, power block, balance of plant, TES, and interest on debt as well as a 30-year plant lifetime [31]. A direct implication of the economics equation on the design is that the aperture area increase causes higher capital costs but could reduce LCOE, if the annual

increase in the amount of useful energy generated exceeds the cost increase. It seems that an increase of the aperture area up to 523,200 m^2 is profitable, as this is where the optimum was found, i.e., at approximately a solar multiple of 2.0.

However, economic analysis must be conducted for the net output of the whole plant. Gross heat collection cannot be considered equal to economic benefit, as an increase of loops results in an increase in the parasitic heat losses of pumps, receivers, and the increased inventory of HTF. The denominator used in LCOE should be the net electrical production during the year, rather than the heat intercepted by the mirrors. In the case of a cold climate site, such a comparison is even more valid since winter protection losses and start-up losses can consume a significant part of time periods with minimum power production.

4. Integrated Design and Supervisory-Control Method

4.1. Design variables and objectives

The integrated design vector is

$$\mathbf{x} = \left[\mathrm{SM},\ H_{\mathrm{TES}},\ T^{\star}_{\mathrm{HTF,out}},\ N_{\mathrm{loop}},\ A_{\mathrm{SF}}\right]^{\mathrm{T}}, \tag{13}$$

where SM is solar multiplier, HTES is storage time, $T^{\star}_{\mathrm{HTF,out}}$ is solar field outlet temperature objective, Nloop is number of loops, and ASF is aperture area. The number of loops and the aperture area are related geometrically since each reference loop corresponds roughly to 3270 m^2 of aperture area. Based on this, the economically optimal size of 523,200 m^2 of aperture area translates to 160 reference equivalent loops. With this change, the aperture size calculation is physically meaningful, and not just a parameter in an optimization problem.

The multi-objective problem is written as

$$\min_{\mathbf{x}}\ \mathbf{F}(\mathbf{x}) = \left[\mathrm{LCOE},\ E_{\mathrm{aux,an}},\ E_{\mathrm{dump,an}},\ R_{\mathrm{winter}},\ -E_{\mathrm{an}},\ -\eta_{\mathrm{sol-elec,an}},\ -\mathrm{CF}\right], \tag{14}$$

where $E_{\mathrm{aux,an}}$ represents the annual auxiliary consumption, $E_{\mathrm{dump,an}}$ is the annual dumped thermal energy, and R_{winter} is a winter-operability constraint. Negative signs are applied in the above objectives since positive signs should be applied where the objective is to maximize. The objectives chosen are purposely intended to avoid having a single objective of efficiency only. An efficient plant might still be unfavorable due to high annual energy, large summer dumping of energy, and poor performance in winter.

A practical winter-operability penalty is

$$R_{\mathrm{winter}} = \sum_{k\in\Omega_{\mathrm{winter}}} \left[\lambda_1 \max(0, T_{\mathrm{safe}} - T_{\mathrm{HTF}}(k)) + \lambda_2 N_{\mathrm{start}}(k) + \lambda_3 P_{\mathrm{trace}}(k)\right]. \tag{15}$$

The first one punishes bad HTF temperature margin safety, the second one punishes frequent start-ups, and the third punishes freeze-protection/heat tracing requirements. Such a term is necessary since a plant working in the cold climate can still be unprofitable regardless of high production during summer months. The penalty ensures that in the process of optimization, more attention will be paid to ensuring continuous winter operation and thermal safety rather than being focused on months when conditions are most advantageous.

The evaluation is conducted using feasible operation decisions and their influence on the time series performance of the plant. That is important since if plant capacity is increased without proper dispatching algorithm, overestimated amount of usable energy can be calculated and underestimated amount of dumped energy. Similarly, optimization of controller on an undersized field may lead to underestimate value of storage since there is not enough surplus thermal energy.

4.2. Operational constraints

The feasible operating region is defined by

$$\mathrm{SM}_{\min} \le \mathrm{SM} \le \mathrm{SM}_{\max}, \tag{16}$$

$$H_{\mathrm{TES,min}} \le H_{\mathrm{TES}} \le H_{\mathrm{TES,max}}, \tag{17}$$

$$T^{\star}_{\mathrm{HTF,out,min}} \le T^{\star}_{\mathrm{HTF,out}} \le T^{\star}_{\mathrm{HTF,out,max}}, \tag{18}$$

$$0 \le E_{\mathrm{TES}}(k) \le E_{\mathrm{TES,max}}, \tag{19}$$

$$T_{\mathrm{HTF}}(k) \ge T_{\mathrm{safe}}, \tag{20}$$

$$W_{\mathrm{PB,min}} \le W_{\mathrm{PB}}(k) \le W_{\mathrm{PB,max}}, \tag{21}$$

$$|\Delta W_{\mathrm{PB}}(k)| \le \Delta W_{\max}. \tag{22}$$

These restrictions enforce the mechanical and thermal disciplines necessary in a real plant. Temperature at the outlet limit ensures safe conditions for HTF and receiver system, temperature energy storage restriction avoids unrealistic energy storage scenarios, and power block restrictions avoid the request of an impossible ramping or low-load scenario by the controller. All these restrictions have economical significance as their violation is represented as an unnecessary generation of energy.

4.3. Predictive supervisory control

The manipulated-variable vector is

$$\mathbf{u}(k) = [\dot{m}_{\mathrm{HTF}}(k),\ Q_{\mathrm{ch}}(k),\ Q_{\mathrm{dis}}(k),\ W_{\mathrm{PB,set}}(k)]^{\mathrm{T}}. \tag{23}$$

The controller solves a receding-horizon problem,

$$\min_{\mathbf{u}(k:k+N_p-1)} J = \sum_{j=0}^{N_p-1} \left[\alpha_1 (W_{\mathrm{ref}} - W_{\mathrm{PB}})^2 + \alpha_2 P_{\mathrm{aux}} + \alpha_3 Q_{\mathrm{dump}} + \alpha_4 \Delta u^2 + \alpha_5 \Phi_{\mathrm{winter}}\right]_{k+j}, \tag{24}$$

subject to the plant constraints and forecasts of DNI and ambient temperature. The tracking term keeps the turbine near useful load, the auxiliary term discourages unnecessary pumping and tracing, the dumping term preserves solar heat when storage has future value, the movement term avoids aggressive actuator changes, and the winter term preserves HTF temperature margin.

It is important to emphasize that the MPC controller does not aim to substitute for the lower-level safety controls. The MPC controller offers an overall supervisory control of field flow, TES charging and discharging, and power block set point. In times of abundance of resources, it allows choosing whether the extra field energy should be directly used or accumulated. During shoulder season fluctuations, it enables damping of field disturbances and minimizing part-load operations. During scarcity in winter, it will choose whether to start up later on the risk of failing to start. The interpretation provided is in line with the MPC literature in general, yet specific to cold-climate trough operation [34,35].

The dispatch runway shown in Figure 4 highlights what data must be on hand for practical purposes: forecasts, storage condition, HTF temperature, load of the power block, auxiliary load, and thermal dump risk. Most importantly, this approach makes clear that the question of storage dispatch is a forecasted opportunity cost problem. Heat sent to the turbine currently cannot be stored for use at night, while heat currently stored in the tank could become waste if there is no further high-DNI event and the storage becomes full before the next DNI peak. Thus, a predictive controller is preferable to a fixed rule in situations where the storage condition can mean something else depending on whether we are in summer, shoulder periods, or winter.

Implementing the controller mentioned here will also require a clear distinction between supervision tasks and process safeguards. While low-level controllers will still need to ensure safe operation of the solar field, HTF pumps, valves, and turbines, the supervisory

optimizer will make decisions above that level, selecting set points based on forecasts of the upcoming solar energy and demand over the next few hours. This hierarchy is important since the optimal dispatch of the plant based on mathematical criteria is meaningless if it causes any thermal-oil limitations, infeasible steam ramp, or premature depletion of storage ahead of a predicted cloud passage.

Figure 4. Predictive dispatch runway.

4.4. Case-study bounds

These limits ensure that the investigation stays close enough to the reference plant without restricting the design variables in exploring the economically viable area. The upper limit on the aperture is set for an area that is slightly bigger than the optimal one, enabling the model to recognize real economic benefits from overbuilding. The lower and upper limits on the temperature at which the fluid leaves the plant are very tight due to the nature of the HTF and steam generation plant (Table 2).

Table 2. Design-space bounds.

Design variable	Unit	Lower bound	Upper bound
Solar multiple, SM	–	1.0	3.0
TES capacity, H_{TES}	h	0	12
Solar-field outlet target, $T^{\star}_{\mathrm{HTF,out}}$	°C	380	400
Solar collector loops, N_{loop}	–	80	200
Solar-field aperture, A_{SF}	m^2	261,600	654,000
Prediction horizon, N_p	h	4	24

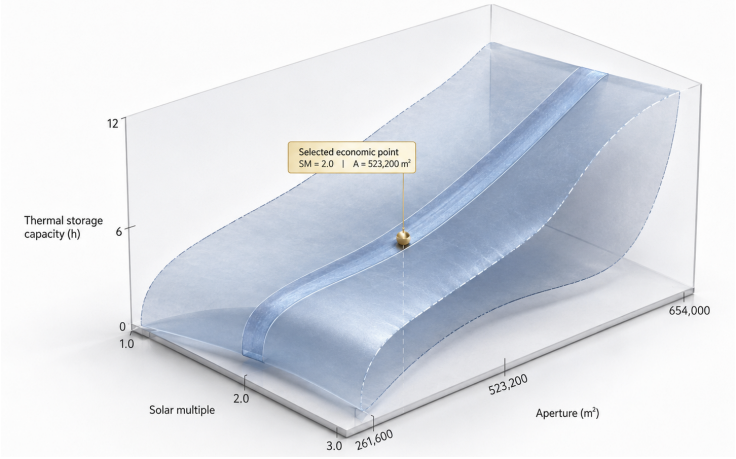

Figure 5. Feasible design corridor.

The feasible design corridor shown in Figure 5 maps out the practical design space. The chosen design point with solar multiple 2.0 and 523,200 m^2 of aperture is situated in a range between two bad design spaces, one of which is the scarcity region and the other of which is the overbuilt region, and both are infeasible due to either insufficient storage charge opportunity or dumping. This information is helpful since it demonstrates that the reported optimal design is a feasible one based on the constraints related to storage hours and outlet temperature.

5. Results and Discussion

5.1. Viability of Design Points and Seasonal Imbalance

In terms of design-point parameters, it becomes clear that the studied CSP plant is thermodynamically viable. Specifically, the efficiency of the solar field (67.4%), power block (35.72%), and solar-to-electric conversion (22.03%) are all plausible for a thermal-oil trough CSP plant under ideal conditions [14]. However, the most remarkable finding here is that the plant's seasonal performance pattern remains quite unbalanced. For instance, while the June day delivers an output of 867.64 MWh, the December day can deliver merely 105.31 MWh. The ratio of these two amounts is equal to 8.24, which exceeds ordinary day-to-day variations.

It follows from above that the shoulder seasons occupy a midpoint between the two aforementioned extremes. Indeed, while March delivers an output of 580.12 MWh, September generates only 511.76 MWh. Hence, March production level is 13.36% higher than the corresponding September production level despite the two months being equally close to the equinox. This implies that seasonal behavior of a CSP plant cannot be explained through mere variations in day length and requires taking DNI, incidence angle, energy storage status, and operational history into account.

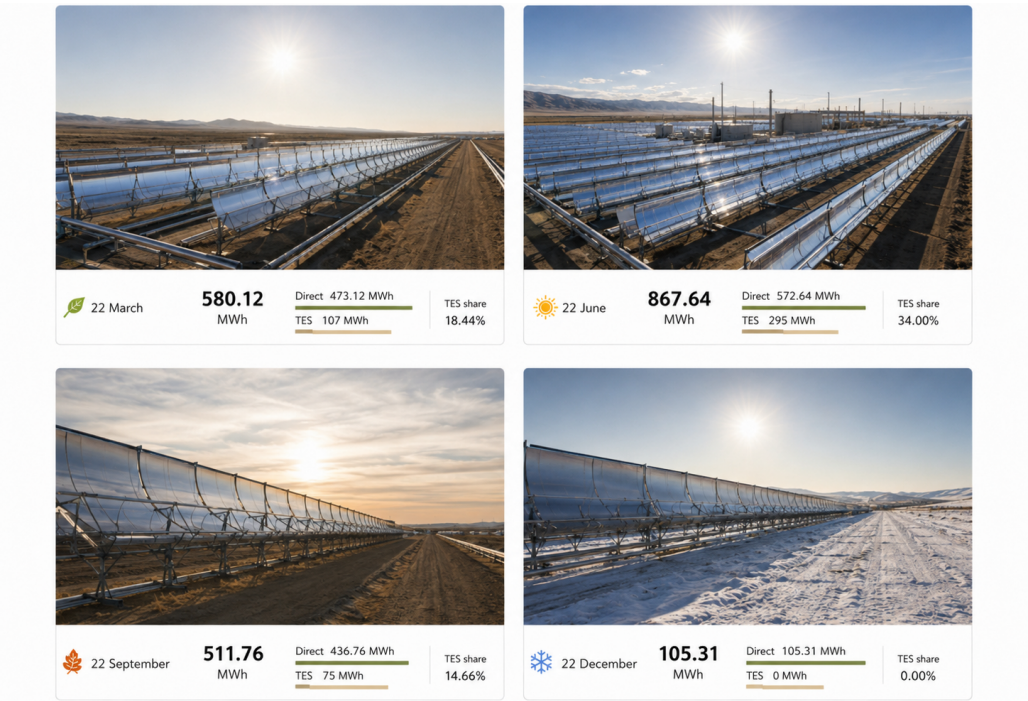

Figure 6. Seasonal energy receipts.

The seasonal energy receipt in Figure 6 distinguishes direct generation and storage-enabled generation, thus revealing the true value of TES. For June, the TES amount to 295 MWh, representing 34.00% of the net daily generation of the plant. For March and September, the TES values represent 18.44% and 14.66% respectively. As for December, no substantial contribution can be expected from the storage as the solar field is unable

to produce enough surplus thermal energy. Hence, this pattern resolves the second part of the research question: storage can only be considered valuable insofar as it receives its initial charge from the solar field. Otherwise, tank capacity does not compensate for lack of charge.

Another useful measure derived from the four-day sample period concerns the capacity factor of the plant. Based on the four representative days, the average daily generation of the plant amounts to 516.21 MWh. Given the plant's rated capacity, this figure corresponds to the sample capacity factor of 43.02%. The above value cannot be interpreted as the actual annual capacity factor as the sample consists of four seasonal days. Nonetheless, the sample CF represents a diagnostic measure. This number indicates the potential for high performance in the case of favorable conditions coupled with the plant's susceptibility to collapse in winter (Table 3).

Table 3. Derived seasonal indicators.

Reference day	Net generation (MWh)	Direct generation (MWh)	TES contribution (MWh)	TES share (%)	Ratio to December
22 March	580.12	473.12	107	18.44	5.51
22 June	867.64	572.64	295	34.00	8.24
22 September	511.76	436.76	75	14.66	4.86
22 December	105.31	105.31	0	0.00	1.00

These new indices thus provide an accounting for the two mechanisms seen visually in the seasonal diagram. The first mechanism is that of direct solar inadequacy: regardless of any impact from storage at all, the amount of direct generation decreases dramatically between summer and winter months. The second mechanism is that of storage augmentation: the largest amount of TES input into the system coincides with that of the largest amounts of direct generation, since thermal energy storage requires extra energy input into the field before storing it. The table thus prevents a possible misunderstanding where storage capacity would be thought of as something entirely separate from field capacity and helpful solely in winter.

Another interesting comparison is provided by the months of March and September. The difference between the total energy production in those months is not significant, but the difference between their shares of energy storage is sufficient to infer different behavior of the process. March has a larger storage share, meaning that either the field produces more extra energy, or that there is a more effective pattern of using stored energy in the power block. September's lower total output and lower storage share indicate that it would be wrong to represent shoulder seasons simply through assumptions about the equinoxes. This is important for control systems design, since a supervisory controller must rely on forecasted daily information, not the season itself.

Finally, the direct generation data make the previous statement clearer. The direct generation in June is 572.64 MWh, or 21.03% larger than the direct generation in March, which totals 473.12 MWh. However, the June total output is 49.56% higher due to the strong storage influence. Thus, the advantages of summer over winter months have been enhanced through thermal energy storage rather than generated independently from it. In September, direct generation reaches 436.76 MWh, almost equal to the March number, but with insufficient storage assistance resulting in lower output. Finally, December, with 105.31 MWh and no useful contribution from storage at all, shows how dispatch flexibility drops away without sufficient field production.

These ratios also illustrate why an annual average would create false impressions regarding the design process. The December day accounts for just 12.14% of the production during June but still needs supervision at the plant level, freezing, circulation, and start-up preparations. When compared on the basis of energy alone, then, the winter case presents a false impression since, even in the winter season, there is need to manage auxiliary systems and thermal risk even with very low energy production levels. The June day is characterized by very high energy production levels as well as high contributions from the storage system, illustrating that the storage benefit increases with more energy in the field than what is needed at the power block.

5.2. Turbine operating performance under part-load exposures

The low production during December suggests that the facility will spend its winter season far below the maximum electric output potential. In terms of a Rankine cycle CSP facility, this is not just a proportional drop in generation. Reduced heat input could lower steam mass flow, raise the share of parasitic loads, prolong startup times, and limit turbine efficiency [21,26,27]. Thus, the impact of such low generation on engineering performance is higher than simple loss of MWh. A day of poor performance may also expose the facility to additional thermal cycling and reduce its readiness for the next productive day.

A storage dispatch controller is able to mitigate this problem by ensuring the protection of power block operating efficiency instead of maximizing instant generation only. A controller which releases excess heat early enough could increase short-term generation at the expense of the capability to provide stable power in the evening. Alternatively, a control mechanism that maintains too high heat level will neglect profitable opportunities for energy production. By using heat storage in the optimal way, one will have smoother and more efficient profile for the power block operations. That is how such considerations are included in a cost function of the supervisor control algorithm.

From the point of view of facility optimization design, the implications seem obvious. If the field size is maintained at the reference value, control will not improve performance during winters and spring-fall periods due to insufficient heat surplus. On the contrary, when the field size is increased without predictive dispatch, the facility will have surplus heat, which could either be dumped or converted sub-optimally. Therefore, integration of control into design should yield higher performance than pure design optimization or dispatch control optimization alone.

The part-load challenge also has a temporal component. A relatively low thermal input at morning hours could be acceptable for the next few hours if DNI is expected to recover rapidly thereafter, whereas a similar thermal input might make sense for postponing the turbine start-up if it was predicted that the DNI window would be short and weak. Thus, the controller needs to determine both how much heat should be sent to the power block as well as when committing the turbine would provide enough net electricity generated to justify the associated auxiliary loads and the need for thermal cycling. For Mandalgobi, this assessment is most important in early winter months and in off-peak periods characterized by an intermittent nature of the solar resource because small variations in the heat generated at the field might make the difference between staying in a feasible regime and operating in a marginal situation.

In this light, the load-quality parameter of the control objective receives its natural interpretation. Rather than being motivated to generate more electricity, the controller should seek maintaining a feasible heat flow through the receiver-HTF circuit, HTF-electricity circuit, and turbine inlet. An optimal dispatch action that appears promising at the field output might become suboptimal for the entire plant boundary because it entails a need for additional pumping, imposes thermal instability to the steam circuitry, or consumes a valuable amount of stored thermal energy before a higher-value period comes. Hence, the right place where one needs to assess the control performance and reward actions is the power block boundary rather than a point further downstream.

This consideration helps to explain why the December day is so important to the system design. Not only because of the mere low energy production rate of 105.31 MWh, but also because of the fact that this day demonstrates the operation mode that is risky in terms of having the power block operate outside of its comfortable load range, and the TES is insufficiently charged to help compensate this deficiency. If it happens repeatedly during winter months, the consequences go far beyond just energy losses and include additional management costs to handle frequent start-ups, increased thermal cycling, and increased freezing demand. Improved load quality in winter can thus save money even if the increase in winter production were not significant.

The capacity tracks in Figure 7 express the four seasonal days in terms of plant-boundary operational quality. The rated capacity of the June day is around 72.30%, com-

pared to the 24-hour rated daily potential, and the December day is just around 8.78%. It should be noted that the blank portions of the tracks represent more than lost energy; rather, they represent hours when the use of fixed auxiliaries, heat rejection system operation, and readiness management is still essential despite the lack of salable electricity generation. Hence, this perspective also reinforces the argument for dispatchability of Mandalgobi based on load quality and thermal continuity, in addition to the MWh output.

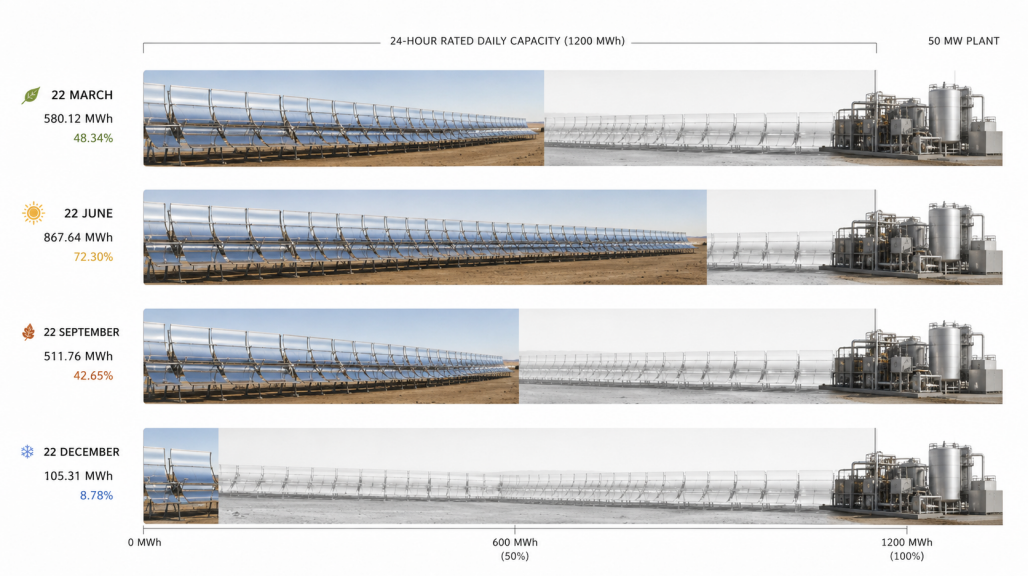

Figure 7. Part-load exposure.

5.3. Sizing of solar fields and economics through LCOE

As stated earlier, the economic optimum occurs at an aperture area of 523,200 m^2, which is twice the reference size of 261,600 m^2. Given that the reference field comprises 80 collector loops, this translates to roughly 160 reference-loop equivalents. This optimal design also comes at the same time with a solar multiple of 2.0 and LCOE of USD 0.2143 kWh^{-1} [31]. This finding is important since it highlights the role of solar field under-sizing in contributing to poor yearly operation.

This is due to the improved capability to achieve efficient operating range conditions during moderately resourceful hours, greater opportunities to recharge the TES with surplus heat after meeting the power block demand, and fewer marginal hours where significant proportion of the generated electricity will go towards the use of auxiliary power. This explains the economic benefit in adding aperture capacity capital cost up to the aforementioned optimum [36].

Field-scale Comparison and Overdesign The field-scale comparison in Figure 8 illustrates the point that overdesign needs to be managed as opposed to installed. Transition from the reference field to the optimum field provides more heat to the plant on beneficial hours, but such heat contributes to improving the plant's LCOE only if used productively through turbine at useful load or stored and dispatched at a later time. Any surplus heat that gets collected and subsequently dumped incurs collection and delivery costs without creating any electricity. Predictive dispatch, therefore, is the means through which the increased aperture is converted into annual electricity production.

In turn, the aperture results provide new direction in the research questions. One does not need to investigate the question of which size field yields more benefits in terms of economics. Mandalgobi analysis suggests that a larger field is needed and solar multiple 2.0 should be considered from the economics perspective. What matters is how the optimal field should be operated in order to use its surplus thermal energy to decrease the amount of times the plant operates at partial loads and increase dispatchability of electricity production.

Aperture as Allocation of Costs Increasing the number of aperture to double (from 80 to about 160 reference-equivalent loops) leads to increase in capital cost due to the larger collector array, receiver surface area, pipes and HTF volume requirements, etc. Thus, the aperture results cannot be explained simply by increasing the energy output alone. They occur due to the optimization of thermal input throughout the year. In simple words, additional capital is spent for the aperture only if the additional aperture increases the frequency of full-load operations and enhances TES capability to generate dispatchable power. This is why LCOE and dispatchability need to be considered together as opposed to two independent factors.

Figure 8. Economic field scale.

The same logic limits excess development of fields. Aperture beyond the minimum economic amount will further increase the instantaneous collection of heat during good weather periods, but the marginal benefit will diminish as soon as the thermal storage is filled, the capacity requirements for turbines are met, or auxiliary pumping exceeds beneficial electricity production. Thus, the optimum found for solar multiple 2.0 cannot be used as an excuse for an unbridled growth of fields. On the contrary, the optimum is proof that for Mandalgobi, a higher aperture will provide better economics, assuming adequate storage and dispatch capabilities.

The comparison of actual and theoretical performance also sheds light on another misconception about the solar multiple concept. There are two definitions of the solar multiple that need to be distinguished. The first, or apparent, solar multiple refers to a ratio based on aperture installed. The second definition, that of effective solar multiple, refers to the share of the total aperture that converts into net output electricity accounting for the losses from thermal conversion, storage and dispatch capabilities, turbine needs, and auxiliary consumption. A cold climate area will experience lower effective solar multiple than apparent during the cold months due to poor incidence, high heat loss, and additional plant protection load. Thus, the presented optimum value can only be considered a point on the dispatch curve, rather than simply an installation scale.

5.4. Coupling of design and control sensitivities

In the context of our analysis, we interpret the field size sensitivity as a form of qualitative sensitivity analysis around the reference design. In the reference scenario, the plant experiences a scarcity of available energy since the field cannot generate enough heat both to run the turbine and charge storage during favorable solar hours. The optimum aperture is a situation where the field has twice the solar collecting area and thus a high chance of generating thermal energy surplus. Further enlargement will only drive up the cost of investment and risks of dumping unless there is some way to utilize the surplus energy. Therefore, the optimum is a specific function of the local site conditions.

The above reasoning helps explain why the control policy is incorporated into the design algorithm. The control law influences the marginal benefit of increasing aperture.

With the possibility of prediction by the controller, the plant can store more energy and thus improve the usefulness of any increased capacity. Conversely, the inability to predict the future demand or the occurrence of scarcity means that an enlarged loop can only lead to an increase in the risk of dumping. In turn, this implies that each loop is valuable for the controller. Finally, design alters the marginal benefit of control. More room is created for the controller to take useful decisions as long as surplus energy is produced by the field.

One sensitivity that is associated with the duration of the thermal storage capacity is the upper bound on improvement of output that storage contributes. As explained previously, an increase in H_{TES} improves dispatch performance as long as the energy surplus is generated and efficiently used by the power block. It is clear that the additional duration contributes to output only if the field has generated some surplus. In other words, the December scenario represents the lower-bound condition. On the contrary, a significant contribution can only occur if the surplus is generated; this applies to the June scenario.

5.4.1. Seasonal value of storage

On the other hand, the TES system plays an essential role in the June scenario. Here, one third of daily generation relies on storage. This is the ideal situation for storage utilization since the solar field can produce enough power to satisfy power-block demand and charge the TES system simultaneously. The amount of storage required by the other months (March and September) is substantially lower, indicating that there is no considerable surplus heat for storage purposes. There is no contribution from TES on the December day due to the lack of recoverable surplus heat.

Thus, the seasonal effect on storage utilization also requires consideration in storage evaluation procedures. A typical annual calculation approach may conclude that larger TES tanks are economically justified since they provide more opportunities for energy shifting. As the example shows, this conclusion may not be valid in the case of cold climates. During winter months, the limiting factor is thermal input into the system, and not tank capacity. In summer months, it may turn into the reverse problem – dispatch decision making and dumping limitation. Finally, during shoulder months, the limiting factor may become storage operation for smoothing purpose. TES capacity should therefore be chosen in conjunction with solar field and control strategy selection and not separately [37].

In addition, it appears that different operating policies may be appropriate for different seasons. In summer, it is beneficial to focus on maximum energy accumulation and release during the night period to prolong the peak power production. In winter, it is critical to avoid thermal stress on components, minimize start-stop cycles, and avoid low-power operation of power block to maintain sufficient efficiency level. For the shoulder months, it is important to ensure stable power delivery without overusing the storage system. Although all of these are possible with one plant design, their implementation strategies depend on the month of the year.

These findings indicate that storage evaluation should take into account not only its capacity but also its operational value. A tank which was never used over the entire winter cannot have any influence on winter dispatchability, despite having a significant energy capacity. The usage of TES tanks during summer can also affect nighttime power generation. However, this effect depends on whether the discharge is performed at the right moment. Thus, the state of charge (SOC) of TES tanks represents not only physical quantity but also an economic opportunity.

March and September examples emphasize this idea further. Despite having nearly identical total generation, the amount of TES energy contribution in September exceeds that in March by 32 MWh. Thus, some of the difference is associated not with the direct production from solar radiation but with its storage. A controller which treats both situations similarly will ignore the distinction. In order to make an optimal choice, a controller needs to consider forecasts regarding solar irradiation and temperature as well as the demand profile in the evening hours.

The storage-opportunity Figure 9 should be seen as a control map rather than the generation map that would otherwise be drawn from it. It says that the same state-of-charge of the TES does not necessarily mean the same choice at any time, since the availability of charge opportunity varies with forecasted irradiance. Partial charging of the tank in summer might be followed by discharging on the same day, because more charge opportunities are expected. Partial charging of the tank in winter might need to be retained for later use, because charge opportunities are scarce and the thermal inventory provides extra margin on temperature. This is exactly what a receding-horizon controller could exploit when forecasting DNI and ambient temperature.

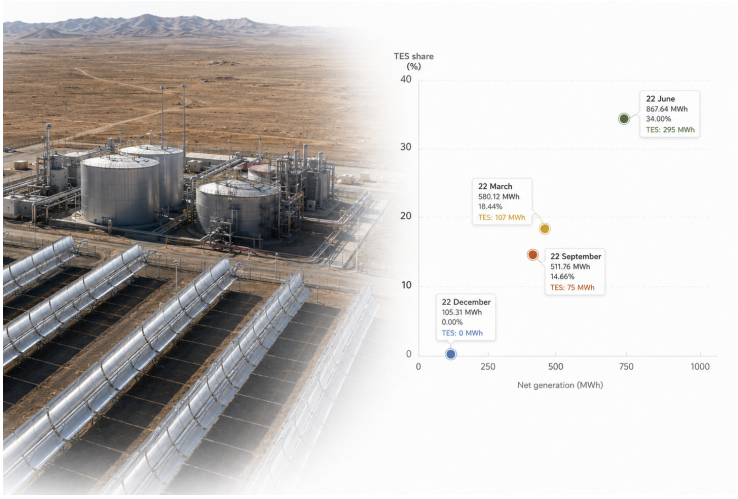

Figure 9. Storage opportunity.

The storage contribution adds an important twist to the notion of reliability. Here, reliability is not just the probability of mechanical availability, but the probability of having sufficient thermal inventory to enable meeting an operating target. In summer, reliability concerns avoiding lost surplus and producing beyond the peak in solar radiation. In winter, reliability concerns retaining temperature margin and avoiding starts that make little sense operationally. Therefore, the same TES plays different roles depending on the season. To see this aspect of TES performance is to recognize its potential for flexibility. Treating TES as a fixed duration does not reveal this aspect, and might even lead to an oversized yet inflexible system.

5.5. Ordering of plant configurations by performance

It is possible to infer four types of plant configurations based on the formulation presented: reference plant design with normal dispatch, increased capacity of the plant without predictive dispatch, reference plant design with predictive dispatch, and increased plant capacity with predictive dispatch. Expected ordering depends on whether or not each configuration resolves either or both structural and operational restrictions. Neither of the configurations for the reference plant resolves additional charging opportunities and prediction for allocating thermal load.

Only the configuration with increased plant capacity and predictive dispatch resolves both issues – it maximizes both heat supply and heat allocation. Therefore, dispatchability for this configuration is expected to perform best, as it makes the plant shift from a scarcity to a surplus regime of production. There is no need to make assumptions about the annual optimization performance for this conclusion, which is inferred from the optimal plant capacity, current shares of energy stored, and penalties at partial loads. An expanded field provides the environment for useful storage, while predictive control dictates whether that storage should be charged, retained, or discharged.

Plate III in Figure 10 represents the final output of the problem based on the engineering thinking involved in the analysis. The base scenario is constrained by seasonal

lack of supply. The design only scenario helps eliminate such constraints but can lead to generation of excess heat during the wrong times. The control only scenario makes better use of the existing heat but still cannot beat inadequate apertures. The integrated approach is the best approach since field dimensions and control periods complement each other. This result is consistent with current CSP practices in which successful plants necessitate coordinated design, commissioning, operations, and maintenance and not just optimal subsystem design [4,9].

Figure 10. Dispatchability answer.

5.6. Engineering implications of cold-climate CSP design

The implications of the Mandalgobi analysis suggest that, as in all engineering problems, the evaluation of cold-climate trough plants should include a distinction between viability and dispatchability metrics. Nominal design-point efficiency will provide the answer to whether a thermodynamic architecture makes sense, but it will not say anything about operational performance through the coldest months. Daily net generation will expose seasonal insufficiency, but it will fail to specify what exactly is lacking – field size, storage volume, turbine part-load performance, or dispatch. TES contribution will clarify whether storage is necessary, but its interpretation requires consideration of charging opportunities. LCOE will identify the optimal field size from an economic standpoint, but only once the control approach has been clearly specified.

For design purposes, the optimal combination of key performance indicators is that of annual energy output, LCOE, storage usage, dumping, auxiliary consumption, capacity factor, start-up rate, and winter availability. It avoids overestimating summer production relative to winter reliability and ensures that storage capacity chosen for annual energy maximization is actually used properly in the off-seasons. A trough plant designed for cold semi-arid climates needs, therefore, to be optimized on both seasonal and annual criteria.

For control, it is essential to understand that predictive dispatch is a fundamental element of CSP technology and cannot be viewed as a merely optional module installed at the end of the installation process. The greater the solar field, the higher its value in case the controller can avoid unnecessary dumping of surplus thermal power and maintain useful storage for critical periods. The larger the storage volume, the higher its economic value if the controller makes use of it to minimize inefficient part load operation and ensure adequate winter thermal margin.

In addition to seasonal availability, there are design issues related to thermal energy storage in CSP plants that should be considered for planning purposes in the Mandalgobi example. Long days can justify storage based on evening electricity production; however, cold climate conditions imply additional issues such as winter preparedness, receiver heat losses, higher HTF viscosity, tracing needs, and startup flexibility. Consequently, a good plant in one location might be undersized and badly operated in another site where different climatic conditions prevail. The comparison that matters here is not between two plant nominal capacities but rather between two plant design operating envelopes.

Another lesson regarding reporting can also be drawn from the above example. In order for a cold climate CSP study to appear convincing, it has to report the following numbers: the capacity, the amount of energy produced annually, the distribution of energy generation throughout the seasons, the proportion of generation which is supported by thermal energy storage, the field size for which costs are minimized, and the scheduling strategy that was applied in operations. This information helps readers judge the capability of the plant to work in an actual dispatchable fashion or to be productive in favorable seasons only.

5.7. Reproducibility, limitations, and validation pathway

The interpretation relies on evidence that consists of measurable quantities in the Mandalgobi plant record and clear calculations like TES share, ratio of June to December production, aperture ratio, and sample capacity factor. These types of evidence enhance the potential for reproducibility since each main conclusion rests on an explicitly stated plant quantity. The subsequent mathematical analysis then describes how the evaluation process would work if hourly weather, the state of the TES, auxiliary power supply, and the dynamic behavior of the power block were available.

To complete a full validation pathway, one would need hourly DNI values, ambient temperatures, wind speeds, plant availability, heat tracing demand profiles, parasitic load functions, start-up energy requirements, the state of charge in the TES, and power-block efficiencies as a function of operating point. With those data available, it would be possible to solve the multi-objective optimization problem directly and to construct plots of Pareto optimal frontiers for levelized cost of electricity, annual net generation, dumped heat fraction, auxiliary power consumption, and winter availability. Preparation for such an analysis is provided in the current paper through the explicit formulation of the decision variables, constraints, objectives, and controls needed in SAM, Modelica, TRNSYS, Ebsilon, or a customized python/matlab-based simulation environment [38].

The principal limitation of this analysis is that only four representative days provide too limited a representation of the weather variability throughout the year. It is not capable of representing sequences of several days without sunlight, equipment failures, slow receiver degradation, and price-responsive dispatch. However, the four-day set is enough to highlight the key asymmetry that any annual optimization would need to account for. If a model cannot match the June-to-December ratio, the uneven TES shares, and the transition from reference aperture to solar multiple 2.0, it will not be reliable for design purposes in cold climates.

6. Conclusions

In this paper, the posed research question was answered in detail through the use of the presented data. According to it, cold-climate CSP plants are governed by two interdependent constraints - the availability of opportunities to charge their storage and the quality of turbine operating regime. Neither the nominal value of storage capacity nor the efficiency of the nominal power generation process can ensure the required performance in winter.

Based on the available dataset, the reference plant exhibits proper design at the specified rated point (67.4% solar-field efficiency, 35.72% power-block efficiency, 22.03% overall solar-to-electric efficiency). However, it experiences a seasonal balance problem

- daily generation varies from 867.64 MWh (June) to 105.31 MWh (December), meaning that the ratio of daily production between summer and winter months reaches 8.24. The contribution of thermal storage is substantial during the summer period (34% in June), becomes insufficient in autumn (18.44% in March and 14.66% in September) and almost disappears in winter (December). Thus, the issue at hand is that the reference plant does not have sufficient recoverable surplus heat to ensure effective charging of its storage during winter.

The economic results confirm the findings above - the minimum LCOE of USD 0.2143 kWh^{-1} is attained near solar multiple 2.0 and aperture area of 523,200 m^2, being twice as much as 261,600 m^2. This outcome suggests that the considered plant has a too small solar field compared to the given seasonal resource pattern. The increase in the aperture area increases opportunities of TES charging and turbine operating near its efficient load point. Nevertheless, such change in solar multiple brings benefits to the economy only if dispatch decisions help to avoid thermal dumping and excessive auxiliary consumption.

The proposed method accounts for both problems in the form of a multi-objective design formulation paired with a forecast-driven supervisory controller. The former defines solar multiple, storage time, temperature target, number of loops and aperture area depending on several parameters (LCOE, annual electricity generation, auxiliary consumption, dumped heat, capacity factor and winter-operability penalty). The latter determines heat transfer fluid (HTF) mass flow rate, TES charge and discharge as well as power block load based on irradiance and temperature predictions. As a result, the plant in question is turned into a dispatchable cold-climate energy system rather than thermally limited one.

It is worth noting that the current answer is determined by the available case-study data. The conclusion would not be as valid in case when the thermal storage ensured a significant winter generation and/or the reference aperture already provided economically optimal conditions. The data from Mandalgobi suggest the contrary - storage plays insignificant role in winter operation, while the most economically attractive field is twice as big as the reference one. Therefore, the proposed plant design follows logically from the plant record rather than any general preference for a more powerful CSP field.

From an engineering perspective, the major outcome of this study concerns the necessity of careful coordination between CSP field sizing and utilization of TES in cold semi-arid regions. Namely, the former will not help to address the seasonal balance problem without increasing the aperture area, and the latter cannot make up for the lack of sufficient surplus heat even with increased area of the field. Hence, the most defendable solution seems to be a CSP plant in which solar field sizing provides sufficient opportunities to charge the thermal storage, TES helps to manage seasonal and intra-day mismatch, while supervisory control ensures turbine efficiency and sufficient thermal margin during winter months.

As for the future developments, the proposed model needs to be applied to an hourly year-long simulation of Mandalgobi site including forecasts of stochastic weather parameters, auxiliary consumption due to start-up fuel consumption and receiver degradation as well as Pareto analysis for multiple objectives including LCOE, winter availability, dumped heat and capacity factor.

References

[1] Change, I. C. (2014). Mitigation of climate change. Contribution of working group III to the fifth assessment report of the intergovernmental panel on climate change, 1454, 147.

[2] Power, C. S. (2010). Technology roadmap concentrating solar power. Current, 5, 1-52.

[3] Răboacă, M. S., Badea, G., Enache, A., Filote, C., Răsoi, G., Rata, M., ... & Felseghi, R. A. (2019). Concentrating solar power technologies. Energies, 12(6), 1048.

[4] Mehos, M., Turchi, C., Vidal, J., Wagner, M., Ma, Z., Ho, C., ... & Kruizenga, A. (2017). Concentrating solar power Gen3 demonstration roadmap. National Renewable Energy Lab.(NREL), Golden, CO (United States).

[5] Price, H., Lu¨ pfert, E., Kearney, D., Zarza, E., Cohen, G., Gee, R., & Mahoney, R. (2002). Advances in parabolic trough solar power technology. J. Sol. Energy Eng., 124(2), 109-125.

[6] Kalogirou, S. A. (2004). Solar thermal collectors and applications. Progress in energy and combustion science, 30(3), 231-295.

[7] Fernández-García, A., Zarza, E., Valenzuela, L., & Pérez, M. (2010). Parabolic-trough solar collectors and their applications. Renewable and sustainable energy reviews, 14(7), 1695-1721.

[8] Turchi, C. (2010). Parabolic trough reference plant for cost modeling with the solar advisor model (SAM) (No. NREL/TP-550-47605). National Renewable Energy Laboratory (NREL), Golden, CO..

[9] Mehos, M., Price, H., Cable, R., Kearney, D., Kelly, B., Kolb, G., & Morse, F. (2020). Concentrating solar power best practices study (No. NREL/TP–5500-75763). National Renewable Energy Laboratory (NREL), Golden, CO (United States); Solar Dynamics, LLC, Denver, CO (United States).

[10] Dudley, V. E., Kolb, G. J., Mahoney, A. R., Mancini, T. R., Matthews, C. W., Sloan, M. I. C. H. A. E. L., & Kearney, D. (1994). Test results: SEGS LS-2 solar collector (No. SAND94-1884). Sandia National Labs., Albuquerque, NM (United States).

[11] Geyer, M., Lüpfert, E., Osuna, R., Esteban, A., Schiel, W., Schweitzer, A., ... & Mandelberg, E. (2002, September). EUROTROUGH-Parabolic trough collector developed for cost efficient solar power generation. In 11th SolarPACES international symposium on concentrated solar power and chemical energy technologies (Vol. 7).

[12] Forristall, R. (2003). Heat transfer analysis and modeling of a parabolic trough solar receiver implemented in engineering equation solver (No. NREL/TP-550-34169). National Renewable Energy Lab., Golden, CO.(US).

[13] Burkholder, F., & Kutscher, C. (2009). Heat loss testing of Schott's 2008 PTR70 parabolic trough receiver (No. NREL/TP–550-45633). National Renewable Energy Laboratory (NREL), Golden, CO (United States).

[14] Wagner, M. J., & Gilman, P. (2011). Technical manual for the SAM physical trough model (No. NREL/TP-5500-51825). National Renewable Energy Laboratory (NREL), Golden, CO (United States).

[15] RP, P., Abdul Baseer, M., Awan, A. B., & Zubair, M. (2018). Performance analysis and optimization of a parabolic trough solar power plant in the middle east region. Energies, 11(4), 741.

[16] Sultan, A. J., Hughes, K. J., Ingham, D. B., Ma, L., & Pourkashanian, M. (2020). Techno-economic competitiveness of 50 MW concentrating solar power plants for electricity generation under Kuwait climatic conditions. Renewable and Sustainable Energy Reviews, 134, 110342.

[17] Ikhlef, K., & Larbi, S. (2020). Techno-economic optimization for implantation of parabolic trough power plant: Case study of Algeria. Journal of Renewable and Sustainable Energy, 12(6).

[18] Teleszewski, T. J., Żukowski, M., Krawczyk, D. A., & Rodero, A. (2021). Analysis of the applicability of the parabolic trough solar thermal power plants in the locations with a temperate climate. Energies, 14(11), 3003.

[19] Montañés, R. M., Windahl, J., Pålsson, J., & Thern, M. (2018). Dynamic modeling of a parabolic trough solar thermal power plant with thermal storage using modelica. Heat Transfer Engineering, 39(3), 277-292.

[20] Schenk, H., Dersch, J., Hirsch, T., & Polklas, T. (2015, September). Transient simulation of the power block in a parabolic trough power plant. In Proceedings of the 11th international modelica conference (Vol. 118, pp. 605-614). Linköping University Electronic Press.

[21] Topel, M., & Laumert, B. (2018). Improving concentrating solar power plant performance by increasing steam turbine flexibility at start-up. Solar Energy, 165, 10-18.

[22] Wang, A., Liu, J., Zhang, S., Liu, M., & Yan, J. (2020). Steam generation system operation optimization in parabolic trough concentrating solar power plants under cloudy conditions. Applied Energy, 265, 114790.

[23] Liqreina, A., & Qoaider, L. (2014). Dry cooling of concentrating solar power (CSP) plants, an economic competitive option for the desert regions of the MENA region. solar energy, 103, 417-424.

[24] Al-Sulaiman, F. A. (2014). Exergy analysis of parabolic trough solar collectors integrated with combined steam and organic Rankine cycles. Energy Conversion and Management, 77, 441-449.

[25] Krishna, Y., Faizal, M., Saidur, R., Ng, K. C., & Aslfattahi, N. (2020). State-of-the-art heat transfer fluids for parabolic trough collector. International Journal of Heat and Mass Transfer, 152, 119541.

[26] Wang, A., Han, X., Liu, M., Yan, J., & Liu, J. (2019). Thermodynamic and economic analyses of a parabolic trough concentrating solar power plant under off-design conditions. Applied Thermal Engineering, 156, 340-350.

[27] Ferruzza, D., Topel, M., Laumert, B., & Haglind, F. (2018). Optimal start-up operating strategies for gas-boosted parabolic trough solar power plants. Solar Energy, 176, 589-603.

[28] González-Portillo, L. F., Muñoz-Antón, J., & Martínez-Val, J. M. (2017). An analytical optimization of thermal energy storage for electricity cost reduction in solar thermal electric plants. Applied Energy, 185, 531-546.

[29] Llamas, J. M., Bullejos, D., & Ruiz de Adana, M. (2017). Techno-economic assessment of heat transfer fluid buffering for thermal ENERGY storage in the solar field of parabolic trough solar thermal power plants. Energies, 10(8), 1123.

[30] Herrmann, U., Kelly, B., & Price, H. (2004). Two-tank molten salt storage for parabolic trough solar power plants. Energy, 29(5-6), 883-893.

[31] Shagdar, E., Lougou, B. G., Sereeter, B., Shuai, Y., Mustafa, A., Ganbold, E., & Han, D. (2022). Performance analysis of the 50 MW concentrating solar power plant under various operation conditions. Energies, 15(4), 1367.

[32] Garcia, C. E., Prett, D. M., & Morari, M. (1989). Model predictive control: Theory and practice—A survey. Automatica, 25(3), 335-348.

[33] Qin, S. J., & Badgwell, T. A. (2003). A survey of industrial model predictive control technology. Control engineering practice, 11(7), 733-764.

[34] Rawlings, J. B., & Mayne, D. Q. (2009). Model predictive control: theory and design, Nob Hill Pub. Madison, Wisconsin, 825.

[35] Camacho, E. F., & Gallego, A. J. (2015). Model predictive control in solar trough plants: A review. IFAC-PapersOnLine, 48(23), 278-285.

[36] Kelly, B., & Kearney, D. (2006). Thermal storage commercial plant design study for a 2-tank indirect molten salt system: Final report, 13 may 2002-31 december 2004 (No. NREL/SR-550-40166). National Renewable Energy Laboratory (NREL), Golden, CO..

[37] Pacheco, J. E., Showalter, S. K., & Kolb, W. J. (2002). Development of a molten-salt thermocline thermal storage system for parabolic trough plants. J. Sol. Energy Eng., 124(2), 153-159.

[38] Ezeanya, E. K., Massiha, G. H., Simon, W. E., Raush, J. R., & Chambers, T. L. (2018). System advisor model (SAM) simulation modelling of a concentrating solar thermal power plant with comparison to actual performance data. Cogent Engineering, 5(1), 1524051.